Construction and Building Materials 309 (2021) 125193

Contents lists available at ScienceDirect

Construction and Building Materials

journal homepage: www.elsevier.com/locate/conbuildmat

Impact of electrodialytic remediation of MSWI fly ash on hydration and mechanical properties of blends with Portland cement

Benjamin A.R. Ebert [a], Mette R. Geiker [b], Wolfgang Kunther [a], Gunvor M. Kirkelund [a,*]

[a] Department of Civil Engineering, Technical University of Denmark, Brovej, building 118, 2800 Kgs. Lyngby, Denmark
[b] Department of Structural Engineering, Norwegian University of Science and Technology, Richard Birkelands Vei 1a, 7491 Trondheim, Norway

ARTICLE INFO

Keywords:
Portland cement
Secondary cementitious materials
Phase characteristics
Reactivity
Thermodynamic modelling
Compressive strength

ABSTRACT

Municipal solid waste incineration (MSWI) residues such as fly ash and air pollution control (APC) residues may serve as new supplementary cementitious materials (SCM). These SCMs may, however, require a pre-treatment to improve material properties. This study investigates the impact of electrodialytically remediated (EDR) MSWI residues to remove heavy metals and salts, on the phase development, setting, and compressive strength development of composite cements with 10 wt% cement replacement, compared to inert quartz or untreated (raw) MSWI residues. All treated MSWI residues showed reactivity in mortar, resulting in higher compressive strength than inert quartz, attributed to additional ettringite and monocarbonate formation. The results indicate that electrodialytical remediation improves the performance of MSWI fly ash in blends with Portland cement, while MSWI APC residues might be used without pre-treatment.

1. Introduction

Portland cement clinker production has been estimated to account for approximately 8% of the global anthropogenic CO_2 emissions, representing a significant environmental issue [1]. Research into replacing Portland cement with other cement types, e.g. belite cement, and magnesium-based cement, is ongoing [2]. However, concrete based on Portland cement clinker is estimated to dominate in the foreseeable future [2]. A well-established strategy for reducing Portland cement clinker use is to partially replace it with supplementary cementitious materials (SCMs). Limited potential for reducing CO_2 emission further with commonly used SCMs such as ground granulated blast furnace slag or fly ash from coal incineration has been identified because of limited supplies of these SCMs [2]. The introduction of new sources of SCMs is therefore needed.

Municipal solid waste incineration (MSWI) residues as fly ash and air pollution control (APC) residues could potentially be a new SCM source [3]. However, MSWI fly ash's chemical composition differs considerably from coal fly ash, suggesting a low potential as an SCM [4]. Untreated MSWI fly ash has a high content of chlorides, sulphates, heavy metals and organic compounds and is considered as hazardous material that is landfilled [4]. On the other hand, landfilling the MSWI fly ash results in the loss of a potential new SCM and valuable metals seen as hazardous in landfills, but if extracted a resource. Furthermore, due to its high content of chlorides, sulphates and metals, MSWI fly ash could be expected to retard the setting [5–8], lower the compressive strength [8] and cause volume expansion [9] of cement-based materials. Various treatment processes to reduce the ashes hazardousness by demobilisation or extraction of metals (e.g. solidification/stabilisation [10,11], milling [12], separation [13,14] or thermal treatments [15,16]) or to improve its use in cement-based materials (e.g. combined phosphonation and calcination [17], melting [18], combined sieving and washing [19] or mechanical chemical stabilisation [20]) have been investigated. Treating MSWI fly ash with these methods have shown promising results when used in cement-based materials, such as increased compressive strength [17–20] and reduced metal leaching [17–19]. However, these treatments do not recover the valuable metals in the ash. A method that can recover the valuable metals, remove soluble salts and improve MSWI fly ash for use in cement-based materials is electrodialytic remediation (EDR) [21,22]. EDR combines electrokinetic remediation and ion-exchange membranes to separate ions from a particulate suspension into different electrolyte solutions, using a low electric current. The metals are released through acidification and migrate as ions in the electric field. EDR does not reduce the concentration of organic contaminants [23]. Partially replacing cement with raw or EDR treated MSWI residue was previously studied by Kirkelund et al. [24]. They

* Corresponding author.
E-mail address: gunki@byg.dtu.dk (G.M. Kirkelund).

https://doi.org/10.1016/j.conbuildmat.2021.125193
Received 17 May 2021; Received in revised form 13 September 2021; Accepted 5 October 2021
Available online 13 October 2021

studied an MSWI air pollution control residue (with flue gas cleaning products) before and after electrodialytic upgrading. They found that mortar made with EDR treated MSWI APC residue achieved higher compressive strength and had reduced metal leaching compared to an untreated APC residue.

Recent research by Ebert et al. [25] identified similarities and differences in the chemical composition of a large dataset of MSWI residues using a principal component analysis. Based on this analysis, one MSWI residue close to; one MSWI residue deviating and one MSWI residue deviating considerably to the average chemical composition of MSWI residues were chosen for electrodialytic remediation at bench-scale [26]. Subsequently, the electrodialytically treated MSWI residues metal leaching when used in cement-based materials was tested for crushed and monolithic mortar [26]. It was found that if a low pH could be maintained during the electrodialytic treatment process, 60 wt% Cd, 80 wt% Cu and 75 wt% Zn could be removed from the investigated MSWI residues and leaching from the mortar containing 10 % electrodialytic treated MSWI fly ash was below the regulatory limits for both monolithic and crushed mortar samples [26].

To further improve our understanding of how EDR treated MSWI residues behaves in cement-based materials, the present study's objective is to determine the impact of EDR of MSWI residues on cement hydration and the development of mechanical properties. The performance is compared to mixtures with an inert material (quartz).

This is accomplished by investigating the development of the hydrate phases with x-ray diffraction (XRD), thermogravimetric analysis (TGA) and thermodynamic modelling, and measuring the development of mechanical properties in the form of initial and final setting time and compressive strength after 1, 3, 28 and 90 days. Thermodynamic modelling of the cement hydration can serve as a powerful tool for further understanding and complements experimental hydration studies and provides a better understanding of the chemical interactions of the solid and aqueous phases during cement hydration and the influence of added SCMs [27]. Thermodynamic modelling has been used to model cement hydration with commonly used SCMs such as blast furnace slag, metakaolin and coal fly ash [27,28]. Thermodynamic modelling has also been used to model the effect of incorporating raw MSWI fly ash in cement pastes and mortar [28] and model the hydration characteristics of ternary blends of raw MSWI fly ash, blast furnace slag and cement. However, it has not been used to investigate the hydration differences between binders with raw or treated MSWI fly ash.

2. Materials and methods

2.1. Materials

Three MSWI residues were in 2018 acquired from two grate fired and one fluidised bed commercial MSWI plants:

1) **Fly ash from Amager Bakke (*Ama*):** A state-of-the-art grate fired incinerator (1680 tons/day) in Copenhagen, Denmark. The facility incinerates household and industrial waste at an average temperature of 1025 °C. The MSWI fly ash sample was extracted before the addition of APC products with an electrostatic precipitator.
2) **Fly ash from Nuuk incineration (*Nuu*):** A grate fired incinerator (40 tons/day) located in Nuuk, Greenland. The facility incinerates household and construction waste at an average temperature of 1060 °C. The MSWI fly ash sample was extracted with an electrostatic precipitator. The facility does not have APC.
3) **APC residue from Ryaverket (*Rya*):** A fluidised bed incinerator (300 tons/day) located in Borås, Sweden. The facility has an average furnace temperature of 900 °C and incinerates household and industrial waste. The APC residue sample was extracted with a textile filter after the APC (a dry scrubber system with lime and activated carbon injection), consisting of fly ash and APC products.

Since the experimental samples were both fly ash and APC residue, the term MSWI residues will be used in this paper when referring to both types of samples. The MSWI residues were treated with EDR using a three-cell bench-scale setup, the treatment method is summarised below, and the treatment details can be viewed in [26]. The MSWI residues used in the bench-scale EDR treatment were first washed three times with deionised water at a liquid/solid ratio of 5. 3 kg of the washed MSWI residue were then mixed with 30 L of deionised water in a stirred container to avoid sedimentation. A constant current of 1 A was then maintained for 28 days to leach and separate the MSWI residues' metals into the electrolyte solutions. The MSWI residue suspension was then filtered through 45 μm filters and dried at 50 °C. The MSWI residue was then crushed manually with a mortar and pestle.

2.2. Preparation of pastes and mortars

Various MSWI fly ashes have already been investigated (untreated and treated), replacing between 5 and 60 wt% cement [29–32]. The previous studies suggest that more than 20 wt% replacement is likely to reduce the strength, and that a 10 wt% replacement is preferable with regard to the limitation of heavy metals as well as chlorides and sulfates [5–8]. Therefore, a 10 wt% replacement was chosen for this study. Paste or mortar with 10 wt% of the raw MSWI residues are denoted *Raw*, while paste or mortar with 10 wt% of the EDR treated MSWI residue are denoted *EDR*.

A Portland cement, inert quartz, sand and a superplasticiser were also used as part of this study.

- The Portland cement was a CEM I 52,5N (MS/LA) consisting of 95–100% Portland cement clinker and 3.7% limestone filler (TGA measurement). Paste or mortar made with 100 wt% cement as a binder are denoted *CEM I*.
- The inert quartz filler was M8 grade quartz, consisting of 99.4 % SiO_2. Paste or mortar made with 10 wt% quartz is denoted *Qua*.
- The sand was CEN standard sand that complies with EN 196–1:2005 [33].
- The superplasticiser was a modified acrylic polymer based on designed performance polymers, with a viscosity of less than 30 MPa, a pH of 6.5 ± 1 and a density of 1.06 ± 0.02 g/cm^3.

The oxide composition (back-calculated from an x-ray fluorescence analysis) and physical characteristics (density and particle size distribution d-values) of the raw and EDR treated MSWI residues, CEM I cement, and quartz used are given in Table 1 and 2, respectively. The inert quartz used is larger than the CEM I cement and its particle size lies within particle size variation of the MSWI residues. The CO_2 content was measured with TGA, using the mass loss between 600 and 750 °C. The relative amount of Cd, Cu, Pb, and Zn, determined with x-ray fluorescence, is given in Table 3, together with the metals' leachable content. The content of leachable metals was determined using the batch

Table 1
Calculated oxide composition and physical characteristics of the raw and treated MSWI residues [26] and CEM I.

		Raw Ama	EDR Ama	Raw Nuu	EDR Nuu	Raw Rya	EDR Rya	CEM I
SiO_2	[Wt%]	4.6	14	6.1	14	6.4	12	20
Al_2O_3	[Wt%]	1.4	2.3	4.6	9.6	4.7	5.3	5.4
Fe_2O_3	[Wt%]	1.0	2.4	0.9	1.4	1.8	2.7	3.8
CaO	[Wt%]	13	28	43	29	42	31	61
MgO	[Wt%]	0.6	0.4	1.4	1.3	1.8	2.2	1.0
SO_3	[Wt%]	34	30	8.9	9.7	8.9	8.7	3.2
K_2O	[Wt%]	14	1.0	12	0.4	2.7	0.7	0.4
Na_2O	[Wt%]	7.4	0.7	22	–	7.0	–	0.3
P_2O_5	[Wt%]	2.6	2.1	1.8	2.7	2.2	3.7	0.3
Cl	[Wt%]	2.8	0.1	24	0.1	13	0.2	0.04
CO_2	[Wt%]	0.0	0.0	2.7	2.4	5.3	2.8	1.6

Table 2
Density and particle size distribution d values of the MSWI residues, CEM I and quartz.

		Raw Ama	EDR Ama	Raw Nuu	EDR Nuu	Raw Rya	EDR Rya	CEM I	Quartz
ρ	[g/cm^3]	2.8	2.7	2.6	2.6	2.5	2.6	3.2	2.7
d_{10}	[μm]	8.7	2.9	1.9	2.4	8.2	2.4	2.7	4.5
d_{50}	[μm]	44	17	13	12	19	11	14	28
d_{90}	[μm]	204	120	49	56	41	130	49	84

Table 3
Relative amount and leachable concentration of Cd, Cr, Cu, Pb and Zn of the raw [25], treated MSWI residues [26] and CEM I.

		Raw Ama	EDR Ama	Raw Nuu	EDR Nuu	Raw Rya	EDR Rya	CEM I
Total								
Cd	[mg/kg]	480	60	420	460	80	100	0.4
Cr	[mg/kg]	300	700	800	1100	400	600	33
Cu	[mg/kg]	1400	520	1300	2000	7900	10,200	140
Pb	[mg/kg]	12,000	31,000	3000	3200	3400	3400	17
Zn	[mg/kg]	55,000	26,000	33,000	41,000	6600	9100	180
Leachable								
Cd	[mg/kg]	430	4.2	0.03	0.01	0.00	0.02	–
Cr	[mg/kg]	1.0	0.1	39	23	0.1	2.6	–
Cu	[mg/kg]	2.6	23	0.4	0.07	52	0.01	–
Pb	[mg/kg]	5.0	4.3	530	0.01	1400	0.00	–
Zn	[mg/kg]	23,000	1700	2.9	0.5	20	0.09	–

leaching test as specified in EN 12457–1 [34].

2.3. Frattini test

The Frattini test was performed per EN-196–5 2011 [35] using 20 g cement or 16 g cement and 4 g MSWI residue or quartz, and 100 ml deionised water at 40 °C. The results are presented as CaO (mmol/l) as a function of OH^- (mmol/l). Included is the saturation concentration curve of the calcium ion (expressed as CaO) as a function of the OH^- concentration, estimated for a 40 °C solution:

$$[CaO] = \frac{350}{[OH^-] - 15} \quad (1)$$

The curve is valid over the range of 45 mmol/l to 90 mmol/l OH^- [35]. Results at or above the solubility curve (zone 2) indicate low to no pozzolanic activity due to saturation with $Ca(OH)_2$. Results below the solubility curve (zone 1) indicate pozzolanic activity due to $Ca(OH)_2$ reduction.

2.4. Setting time

The cement paste for the setting time test was prepared per EN 196–3:2009 [36] with the following deviations. 500 g of cement (Ref) or 450 g + 50 g quartz or MSWI residue were mixed with 250 g of deionised water. The mixing process used follows the procedure outlined in EN 196–1:2005 [33], instead of EN 196–3:2009 [36], with cement added to a 5-litre stainless steel bowl first and then mixed with deionised water. For the paste with 10 wt% admixture and cement, the admixture and cement were mixed for 2 min before adding water.

The initial and final setting time of the cement paste and paste with MSWI residue or quartz were determined per the method specified in EN 196–3:2009 [36] using an automatic Vicat apparatus Matest E044N Vicatronic. The mould was not inverted during the test after the initial setting had been measured as specified in EN 196–3:2009 [36].

2.5. Phase development

The cement paste used for the phase development assessment was prepared using the quantities for setting time determination. However, the paste was mixed using a high shear mixer (Whip Mix Power Mixer Model B). The paste was first mixed manually for 30 s, then left to rest for 30 s and finally mixed for 180 s with the high shear mixer. The paste samples were then cast in 18 ml (27.1 mm diameter) Nalgene LDPE sample vials with snap closure and stored sealed at 20 °C and greater than 90% relative humidity. Paste samples were only repeated once per date tested.

The pastes' hydration was stopped after 1, 3, 28 and 90 days using a three-step procedure with isopropanol and diethyl ether, as described in [37]. Several slices (approximately 2 mm thick) were cut from the middle part of the paste sample and crushed in a porcelain mortar to a particle size below 1 mm. Approximately 4 g of crushed paste was immersed in 67 ml isopropanol, shaken for 30 s and left to rest for 5 min before decanting the isopropanol. This step was performed twice. After the second washing with isopropanol, the sample and isopropanol were vacuum-filtered. The crushed paste was then immersed in 13 ml diethyl ether, shaken for 30 s and left to rest for 5 min before vacuum-filtering the solution. The crushed paste was then dried at 40 °C for 8 min to remove any remaining ether, the crushed paste was then ground to a particle size below 63 μm.

2.5.1. X-ray diffraction

The crystalline phases in the crushed paste were identified with XRD. A Pan Analytical x-ray diffractometer equipped with a PW3064 Spinner stage was used for the measurements. The x-ray source was Cu-Kα with a wavelength of 1.54 Å. The crushed paste was backloaded into the sample holder and measured between 4° 2θ – 100° 2θ. The step size and sampling time per step were 0.002°2θ and 24.8 s, respectively. The crystalline phases were identified from the XRD plots by comparing the pure crystalline phase plots shown in Table 4 in conjunction with the ICDD PDF4 database.

2.5.2. Thermogravimetric analysis

Thermogravimetric analysis (TGA) was performed with a NETZSCH STA 449 F3 Jupiter to assess the bound water and portlandite content in the paste samples. Approximately 50 mg of the crushed paste was placed into 85 μl aluminium oxide crucibles (diameter 6.8 mm). The weight loss was measured from 29 °C to 900 °C, a heating rate of 10 °C/min, in a nitrogen atmosphere (50 ml/min of nitrogen gas was used as purge gas). The results were analysed using the Proteus Analyzer software. The crushed paste's bound water content was determined as the mass loss

Table 4
Crystalline phases and corresponding ICSD and PDF number.

Name	Formula	ICSD number	PDF number
Alite M3	Ca_3SiO_5	94,742	85–1378
Alite M	Ca_3SiO_5	81,100	42–551
Belite β	Ca_2SiO_4	81,096	33–302
C_3A cub.	$Ca_3Al_2O_6$	1841	38–1429
Brownmillerite	$Ca_2Al_{1.35}Fe_{0.651}O_5$	98,839	01–074-3675
α-Quartz	SiO_2	174	46–1045
Anhydrite	$CaSO_4$	15,876	37–1496
Bassanite	$CaSO_4$•0.5(H_2O)	79,529	41–224
Gypsum	$CaSO_4$•2(H_2O)	409,581	33–311
Calcite	$CaCO_3$	73,446	5–586
Portlandite	$Ca(OH)_2$	202,220	4–733
Ettringite	$Ca_6Al_2(SO_4)_3(OH)_{12}(H_2O)_{26}$	155,395	41–1451
Friedel's salt	$Ca_2Al(OH)_6Cl(H_2O)_2$	62,363	01–078-1219
Hemicarbonate	$Ca_4Al_2(OH)_{12}(OH)(CO_3)_{0.5}(H_2O)_5$	–	41–0221
Monocarbonate	$Ca_4Al_2(OH)_{12}(CO_3)(H_2O)_5$	59,327	01–087-0493

between 50 °C and 550 °C (H_2O_g). The portlandite content was determined based on the mass loss between 400 °C and 550 °C (H_2O_g) using tangential quantification to exclude any C-S-H loss [37]. The portlandite content was calculated using the molar masses of portlandite and water. The results were normalised as mass relative to the mass of the anhydrous binder in the paste (weight at 550 °C).

2.5.3. Thermodynamic modelling

The Gibbs free energy minimization program (GEMS) [38] was used to model the cement paste phase development as a function of the % of reacted MSWI residue. The program computes equilibrium phase assemblages and speciation in complex chemical systems. The standard PSI-GEMS database in GEMS was supplemented with the CEMDATA18 database [39]. The C-S-H phase was modelled using the CSHQ model proposed by Kulik [40]. The databases used do not account for heavy metals, such as Zn or Pb, on the resulting phase assemblage. The following phases were excluded from the modelling: M−S−H, Al$(OH)_{3am}$, Al$(OH)_{3mic}$, gibbsite, graphite, C_3AH_6, anhydrite, thaumasite, iron, hematite, magnetite, geothite, quartz and silica-amorph. The MSWI residues and CEM I cement input was calculated from the XRF results as listed in Table 1, scaled so that the oxides shown were equal to 100 wt%. For the performed calculations, a reaction degree of 80% was used for the cement without accounting for the differences in the different clinker phases degree of reaction.

2.6. Compressive strength

Mortar prisms (4x4x16 cm^3) for compressive strength testing were prepared per EN 196–1:2005 [33]. The CEM 1 sample was made with 450 g cement, 225 g deionised water and 1350 g CEN standard sand. Mortar with 10 wt% cement replacement was made with 405 g cement, 45 g MSWI residue or quartz, 225 g deionised water and 1350 g CEN standard sand. Superplasticiser was added to the deionised water for mortar prisms made with the MSWI residues to maintain a consistency equal to the CEM 1 and Qua mortar's consistency, as determined by the fall table test EN 1015–3: 1999 [41]. Superplasticiser was added to the mortar with Raw Ama (5.4 g), Raw Nuu (0.3 g), Raw Rya (0.5 g), EDR Ama (1.4 g), EDR Nuu (1.5 g) and EDR Rya (1.3 g). The prism moulds were filled with mortar halfway and vibrated for 15 s at 50hz, then filled over the following 15 s and finally vibrated for a total of 120 s. The prisms were stored covered in their moulds for 24 h at 20 °C and ~ 90% relative humidity. After 24 h, the prisms were demoulded and submerged in containers with a solution of 3 g $CaOH_2$ per litre deionised water until testing. The prisms from the different mortar mixtures were stored in separate containers. The mixes for the CEM I mortar and mortar with quartz was repeated 3 times per date tested.

The compressive strength of mortar prisms was measured after 1, 3, 28 and 90 days of curing per EN 196–1:2005 [33]. All samples were tested perpendicular to the casting orientation after splitting the prisms in two with an electro-mechanic test machine (Instron 6025, 100 kN) followed by compressive strength testing with the Instron 6025 or a Toni Technik 300 ton compression test machine. The as measured compressive strength (σ) was normalised to the air free compressive strength (σ_0), using the equation by Osbæck [42]:

$$\sigma = \sigma_0 - e^{-\varphi \bullet p} \tag{2}$$

The air content (p) of the mortar, after one day of curing, was determined using an indirect method, based on the difference in density of the mortar immediately after demoulding (ρ) and the theoretical mortar density (ρ_0), according to the equation by Osbæck [42]:

$$p = 1 - \frac{\rho}{\rho_0} \tag{3}$$

The density of the mortar prism's was calculated immediately after demoulding based on the difference in weight (w_{ow}) above water and submerged in water (w_{uw}), and the density of water (ρ_w):

$$\rho = \frac{w_{ow}}{w_{ow} - w_{uw}} \bullet \rho_w \tag{4}$$

The theoretical density of the mortar was calculated based on the density and mass of the mortar ingredients:

$$\rho_0 = \frac{m_c + m_s + m_w + m_a}{\frac{m_c}{\rho_c} + \frac{m_s}{\rho_s} + \frac{m_w}{\rho_w} + \frac{m_a}{\rho_a}} \tag{5}$$

Where m_c and ρ_c is mass and density of the cement, m_s and ρ_s is the mass and density of the sand, m_w and ρ_w is the mass and density of water and m_a and ρ_a is the mass and density of the admixture. The measured air content is an indication of the macroporosity of the mortar prisms.

3. Results and discussion

3.1. Impact of EDR on MSWI residue composition and pozzolanic reactivity

The general changes to the oxide composition and Cl after the electrodialytic remediation treatment were reduced K_2O, Na_2O and Cl concentrations and an accumulation of SiO_2, Al_2O_3 and Fe_2O_3, see Table 1. A reduced concentration of CaO could be observed for EDR Nuu and EDR Rya, while EDR Ama had an increased CaO concentration. Furthermore, EDR Nuu and EDR Rya had an accumulation of SO_3, while EDR Ama had a 4% reduction in SO_3. Previous work by Ebert et al. [25] found that Raw Nuu and Raw Rya contained 1.9 wt% and 6.0 wt% water-soluble Ca^{2+}, and 0.6 wt% and 0.2 wt% water-soluble SO_4^{2-} respectively, while raw Ama contained 0.1 wt% water-soluble Ca^{2+} and 21 wt% water-soluble SO_4^{2-}. Therefore, the EDR treatment would have removed low amounts of Ca^{2+} compared to SO_4^{2-} from Raw Ama while removing high amounts of Ca^{2+} compared to SO_4^{2-} from Raw Nuu and Raw Rya.

Other work by Ebert et al. [26] also showed that the raw MSWI residues contained $CaSO_4$, NaCl, KCl and $CaCO_3$. Raw Ama also contained other SO_4 bearing phases, such as $NaSO_4$, and no $CaCO_3$, while Raw Rya also contained CaClOH. After the EDR treatment, $CaSO_4$, $CaSO_4{\cdot}2H_2O$ and $CaCO_3$ were found in EDR Nuu and EDR Rya, while EDR Ama contained $CaSO_4$, $CaSO_4{\cdot}0.5H_2O$ and $PbSO_4$. Therefore, the treatment process reduced the K_2O, Na_2O, Cl and SO_4^{2-} (Raw Ama) content by removing NaCl, KCl, CaClOH (Raw Rya) and $NaSO_4$ (Raw Ama). The high CaO and SO_3 observed in the treated MSWI residues could result from $CaSO_4{\cdot}0.5H_2O$, $CaSO_4{\cdot}2H_2O$, $PbSO_4$ formation and $CaCO_3$ accumulation. However, EDR Nuu and EDR Rya had reduced concentrations of CO_2. Their CO_2 content was measured with TGA, see

[26], as the mass loss occurring around 650–750 °C, and were interpreted as CO_2 bound in $CaCO_3$, potentially indicating a reduction in $CaCO_3$ after EDR.

Reduced K_2O, Na_2O and Cl concentrations are desirable for cement-based materials due to the risk of alkali-silica reactions and reinforcement corrosion [26]. The requirement for coal fly ash used as an SCM is less than 5 wt% Na_2O_{eq} [43], which the treated MSWI residues are within. However, the requirement for Cl is 0.01 % [43], which the treated MSWI residues exceed by a magnitude of 10. An increase of SiO_2-Al_2O_3-Fe_2O_3 is desired as these are the pozzolanic reactive oxides in SCMs [44]. The requirement for coal fly ash is $\sum SiO_2$-Al_2O_3-$Fe_2O_3 \geq 70$ wt% [43]. The sum of SiO_2-Al_2O_3-Fe_2O_3 in EDR Ama, EDR Nuu and EDR Rya was less than 25 wt%. Therefore, it was expected that the treated MSWI residues were not as pozzolanic as coal fly ash. Fig. 1 depicts the raw and treated MSWI residues in a CaO-Al_2O_3-SiO_2 ternary diagram.

Raw Nuu and Raw Rya had CaO-Al_2O_3-SiO_2 ratios close to limestone, while Raw Ama had a ratio matching Portland cement. After the EDR treatment, the treated MSWI residues had ratios similar to Portland cement. Therefore, the MSWI residues may be categorised as high-Ca mineral additions.

Fig. 2 shows the results of the Frattini test characterising pozzolanic reactivity. All MSWI residues were within zone 2, indicating no pozzolanic activity, as suggested by their low SiO_2-Al_2O_3-Fe_2O_3 content. However, only the cement paste with Raw Nuu was within the area specified by the test.

The cement paste with Raw Ama was highly saturated with OH^- (256 mmol/l after 8 days), while the Ca^{2+} had been consumed (3 mmol/l after 8 days). In contrast, the paste with Raw Rya was undersaturated with OH^- (41 mmol/l) and oversaturated with Ca^{2+} (25 mmol/l). Extended hydration time reduced the Ca^{2+} and OH^- content, except for Raw Ama, where OH^- increased to 266 mmol/l after 15 days. Some phases in these two raw MSWI residues could have reacted with the hydrochloric acid and EDTA solutions, interfering with the results.

Although the pastes with treated MSWI residue did not show any pozzolanic reactivity, the results shifted towards zone 1 after 15 days, more than the quartz paste, potentially indicating slow reactivity.

The EDR treatment did not reduce the relative amount of heavy metals in the MSWI residues, increasing the relative amount instead, except for Cd, Cu and Zn from Raw Ama, see Table 3. This may be attributed to removing the previously discussed phases with high solubility (e.g. KCl, NaCl and Na_2SO_4), resulting in an increase in the relative amount of the studied heavy metals, despite removing part of the metals.

Previous experiments have shown that the MSWI residues contain compounds that may accelerate or retard hydration [47]. The impact of different components is briefly summarised in Table 5.

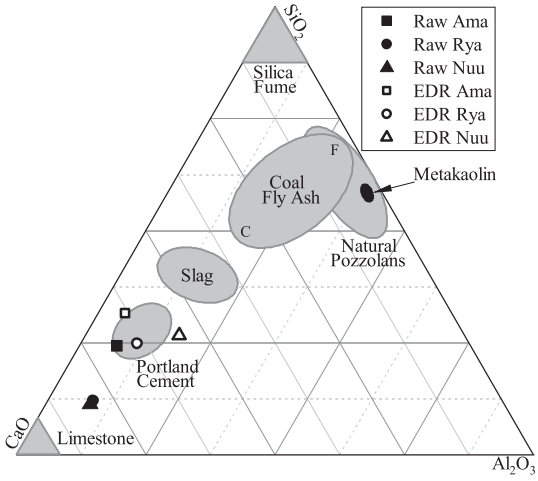

Fig. 1. CaO-Al_2O_3-SiO_2 ternary diagram, with the ratios of the raw and EDR treated residues compared to Portland cement and selected SCMs from Lothenbach et al. [45] and Thomas et al. [46]. C: High calcium coal fly ash, F: Low calcium fly ash.

The present study's raw MSWI residues contained compounds that could make them function as hydration accelerators, e.g. $CaCO_3$, NaCl, or Na_2SO_4. However, given the MSWI residues high content of heavy metals, they could retard the hydration instead if the blended binders metal concentration is high enough. Although the EDR treatment did not reduce the relative amount of heavy metals as intended, this may not be a problem when using the treated MSWI residues. Previous research by Kirkelund et al. [61] suggests that metal leaching after EDR is reduced and does not affect the blended binders' compressive strength as drastically as raw MSWI residues when compared to a 100 wt% cement sample. As indicated in Table 3, the studied MSWI residues leach less in deionised water after EDR, which would also imply the lower reactivity of heavy metals in the cement blends.

3.2. Hydration and phase development

3.2.1. CEM I and quartz paste

Fig. 3 combines the XRD diffractograms of the CEM I and quartz cement pastes. The cement pastes without MSWI residues showed a decreasing peak intensity of the initial Portland clinker phases alite (A), belite (Be), tricalcium aluminate (Ta) and brownmillerite (Br) from 1 to 90 days of hydration. The crystalline phases formed after 1 day of hydration were portlandite (P) and ettringite (E), followed by hemicarbonate (H) after 3 days, and monocarbonate (M) after 28 days. The continued reaction of tricalcium aluminate in cement paste after gypsum has been consumed would, under different conditions, lead to the destabilisation of ettringite and the formation of monosulphate. However, in the presence of limestone, hemicarbonate and monocarbonate form instead of monosulphate, stabilising ettringite [62,63]. Experimental studies have shown that hemicarbonate is initially formed [54], which may be due to the slow dissolution of limestone at high pH [9].

The results of the quantification of bound water and portlandite content with TGA are shown in Fig. 4. The CEM 1 paste and paste with quartz had an increasing content of bound water and portlandite, as suggested by decreasing peak intensity of the initial clinker phases with XRD. The cement paste with quartz had the same bound water and portlandite development over time as the CEM I paste, albeit at a reduced quantity due to the reduced cement content. After 90 days, the CEM I paste contained 31 wt% bound water, while the paste with quartz contained 29 wt%. The portlandite content in the CEM I paste and paste with quartz was 23 and 22 wt%, respectively.

3.2.2. Raw MSWI residues

Fig. 5 shows the XRD diffractograms and thermodynamic modelling results of the cement pastes with Raw Ama, Raw Nuu and Raw Rya. The pastes with Raw Ama or Raw Nuu had peaks of alite (A), belite (Be), tricalcium aluminate (Ta) and brownmillerite (Br) with high intensity compared to the Qua paste after 1 day of hydration, suggesting that the cement was largely unhydrated after 1 day. This is further evidenced by the low intensity of the portlandite peak, indicating that only a small amount of alite had reacted after 1 day. However, the paste with Raw Nuu had portlandite peaks with higher intensity than the paste with Raw Ama, suggesting a higher degree of reaction after 1 day. Ettringite (E) was present after 1 day of hydration, indicating that the aluminate/ferrite phases react partially.

Furthermore, gypsum (G) peaks could be found in the paste with Raw Nuu, indicating an excess of sulphate after 1 day of hydration, suggesting either a lower degree of reaction than paste with Raw Ama or that the tricalcium aluminate reaction is retarded. Raw Ama and Raw Nuu contained compounds that could have accelerated the hydration, e.g. NaCl, KCl or Na_2SO_4. In large concentrations (36 % NaCl and 34 % KCl by mass of water), NaCl and KCl have been shown to retard class G cement [7]. At the cement level replaced in this study (10 wt%), the concentration of Cl was too low (less than 3 wt%) to retard the setting

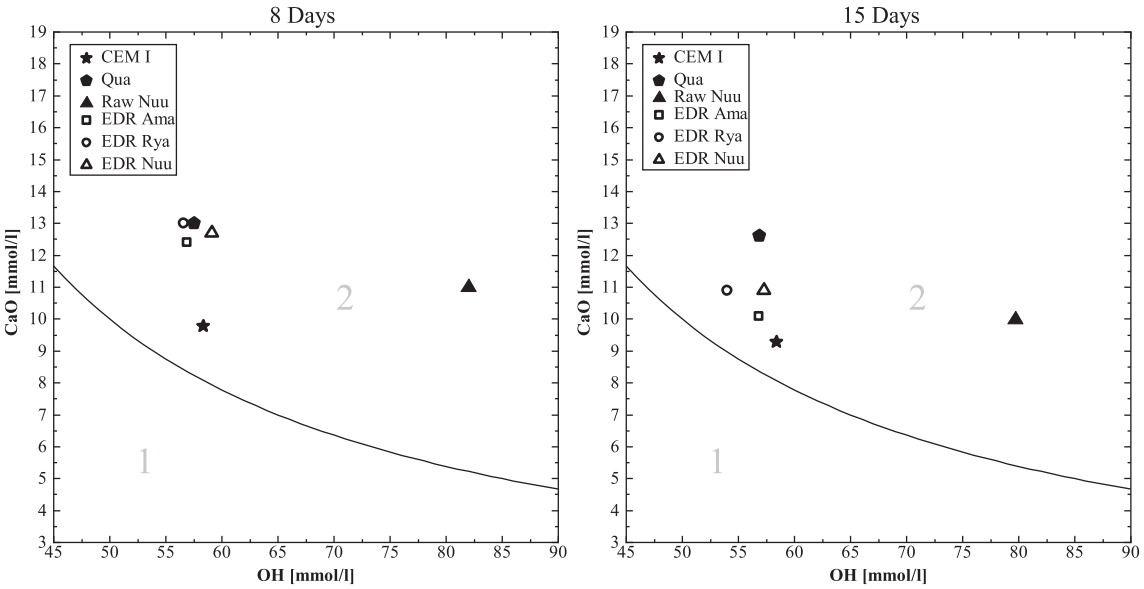

Fig. 2. Frattini test results for the CEM I paste, and paste with quartz and the MSWI fly ash residus after 8 days (left) and 15 days (right).

Table 5
Components influencing hydration reactions.

Element/ compound	Main hydration effect	Described effects
Alkalis	Acceleration	May accelerate alite hydration leading to higher early strength but less strength at later ages [48,49].
$CaCO_3$	Acceleration	Leads to hemicarbonate and monocarbonate formation. May accelerate hydration due to nucleation and dilution effects [48,49].
Cl^-	Acceleration	$CaCl_2$ is a commonly used accelerator that reduces the initial and final setting due to C-S-H supersaturation [50–52]. NaCl may accelerate alite and aluminate hydration (class G cement) [7,53]. More 20–36 % NaCl and 34% may retard instead [7,53].
SO_4^{2-}	Acceleration	Na_2SO_4 and $CaSO_4$ may accelerate hydration, increasing alite hydration during the first days. Gypsum may lengthen the induction period while increasing the hydration rate in the acceleration period. [6,48,54]
Cd^{2+}	Retardation	Cd may or may not retard setting time. 0.18 mol Cd^{2+}/kg binder may delay setting by 3 h. It may also reduce the compressive strength [8,55].
Cr^{3+}	Retardation	Cr(III) may significantly hinder C-S-H and CH formation after 1 day while leading to accelerated CH growth after 31 days [56].
Cu^{2+}	Retardation	Cu may result in large variation in setting time. 0.18 mol Cu^{2+}/kg binder may delay setting by 98 h. Low levels of Cu may increase compressive strength while high levels reduce compressive strength [8,55,57].
Pb^{2+}	Retardation	Pb may coat cement clinker and block hydration, causing a drop in strength. 0.18 mol Pb^{2+}/kg binder may delay setting by 23 h. Reasonably normal hydration reactions occur after 3 days delay with less C-S-H and CH after 28 days. Small quantities may accelerate setting [8,55,57–59].
Zn^{2+}	Retardation	It has been reported that 0.18 Zn^{2+} mol/kg binder delays setting by 360 h. The retardation has been shown to have no long-term effect on the product quality. Low Zn levels may increase strength, while higher levels inhibit strength [8,57,60].

and would have been expected to accelerate hydration instead.

Therefore, the reduced degree of reaction after 1 day could have been caused by the MSWI residues' metal content. Raw Ama had a high relative amount of Pb (12000 mg/kg) and Zn (55000 mg/kg), while Raw Nuu had a high relative amount of Zn (33000 mg/kg). The potential accelerants in the two fly ashes may then have helped offset the hydration delay. The delayed early hydration is easily observed with TGA (Fig. 4), as the pastes with Raw Ama and Raw Nuu had between 5 and 10% bound water and 1% $Ca(OH)_2$ after 1 day of hydration, compared to 14% bound water and 12% $Ca(OH)_2$ in the Qua paste. During the 1–90 days of hydration, alite, belite, tricalcium aluminate, and brownmillerite's peak intensities were reduced. However, after 90 days of hydration, they remained visible, compared to the Qua paste, suggesting that the degree of reaction was reduced. This is corroborated by the TGA, as the amount of bound water and portlandite measured after 90 days were less than the paste with quartz. The paste with Raw Nuu did contain more portlandite than the paste with Raw Ama, suggesting a higher degree of reaction in the paste with Raw Nuu after 90 days, despite binding less water. This may be due to lower amount Zn in Raw Nuu. Monocarbonate (M) was not detected with XRD in the pastes with Raw Ama or Raw Nuu. Only hemicarbonate (H) formed in the paste with Raw Ama (barely detectable), while Friedel's salt (F) formed in the paste Raw Nuu. The results of the thermodynamic modelling support this observed phase development. Monocarbonate would be below the XRD detection limit (2 %) if more than 30% of Raw Ama reacted, forming ettringite instead due to its high SO_3 and low Al_2O_3 content, while Friedel's salt would be the only detectable phase if more than 32 % of Raw Nuu had reacted, due to the high Cl content. The difference in bound water content between the pastes with Raw Ama and Raw Nuu after 1 and 3 days of hydration could be due to a higher ettringite content in the paste with Raw Ama.

In contrast, the cement paste with Raw Rya had similar peak intensities for the initial clinker phases after one day of hydration as the 100 wt% CEM I and Qua pastes and had the highest amount of bound water after 1 and 3 days of hydration together with a similar portlandite content as the paste with quartz. Furthermore, after 90 days of hydration, the peak intensities remained similar to the CEM I, suggesting that Raw Rya does not inhibit hydration and contained more bound water than the paste with quartz. Raw Rya contains fewer heavy metals than Raw Ama and Raw Nuu and has a relative amount of Zn of 9100 mg/kg. Raw Rya does have a high relative amount of Cu (10200 mg/kg). However, at 10 wt% cement substitution, the concentration of Cu in the

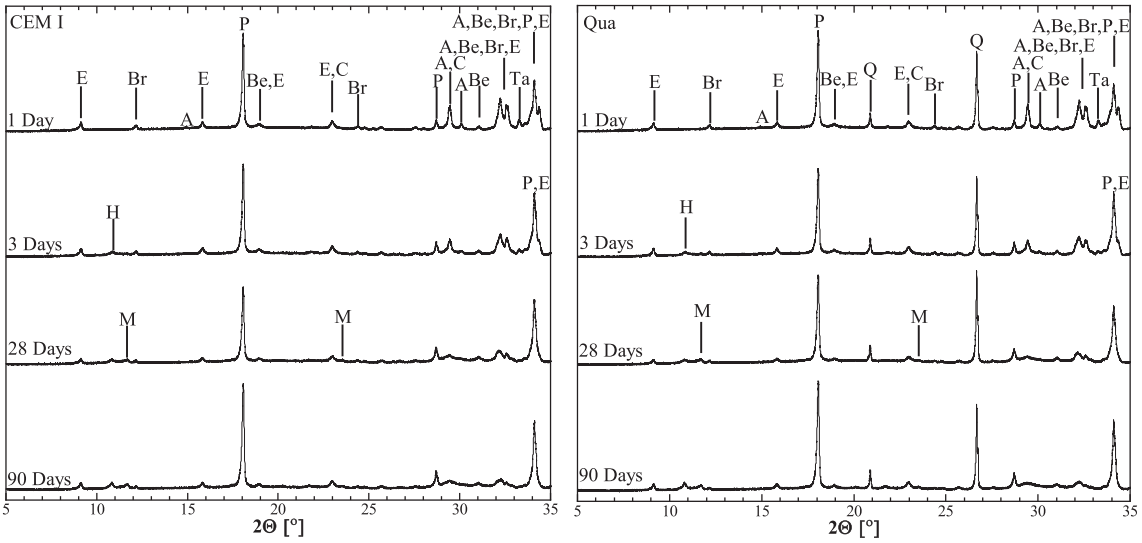

Fig. 3. XRD patterns for the CEM I (left) and quartz (right) pastes cured 1, 3, 28 and 90 days. Alite (A), belite (Be), tricalcium aluminate (Ta), brownmillerite (Br), portlandite (P), ettringite (E), hemicarbonate (H), monocarbonate (M), calcite (C) and quartz (Q).

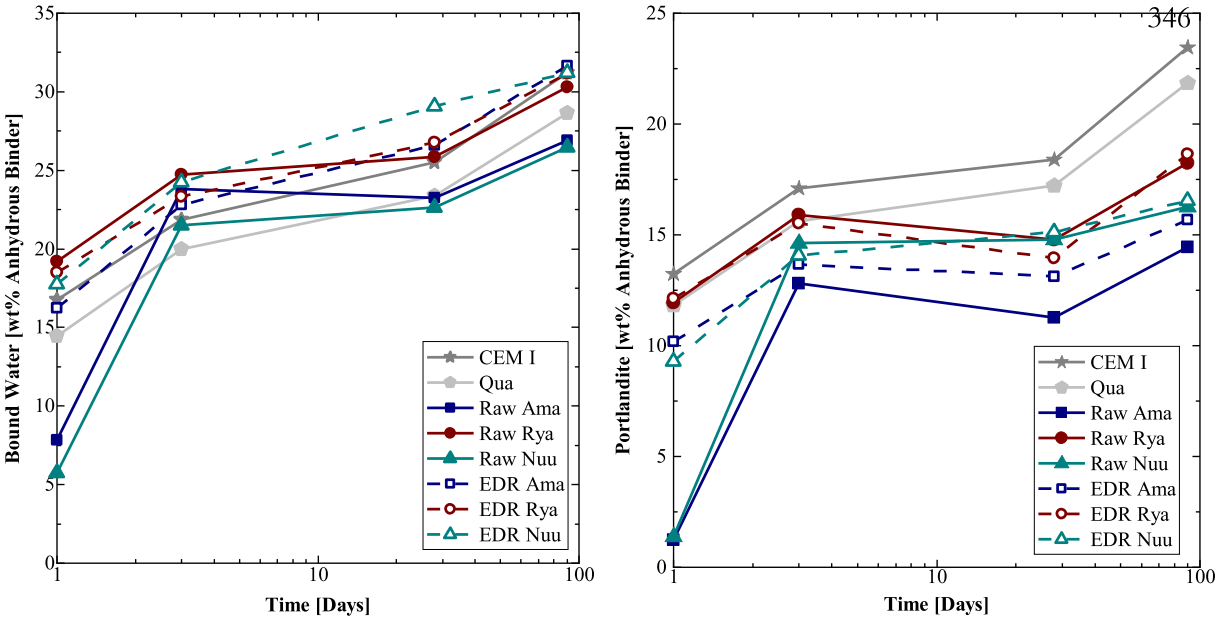

Fig. 4. Bound water and portlandite content as wt% of the experimental pastes.

paste may be low enough to have a beneficial effect instead of a detrimental effect on hydration. The paste with Raw Rya formed Friedel's salt instead of monocarbonate, similarly to Raw Nuu. The thermodynamic model results confirm this by favouring Friedel's salt formation instead of monocarbonate with an increasing percentage of reacted ash. Similarly to the paste with Raw Nuu, if more than 32% of the ash has reacted, monocarbonate can not be detected with XRD. As the portlandite content measured with TGA was similar to the paste with quartz after 1 and 3 days, the increased bound water is likely, not due to additional C-S-H but due to increased ettringite and the formation of Friedel's salt. The pastes with Raw Ama and Raw Rya both had a reduction in portlandite content between 3 and 28 days of hydration, which may indicate some form of portlandite consumption.

3.2.3. EDR treated MSWI residues

Fig. 6 shows the XRD diffractograms and thermodynamic modelling results of the cement pastes with EDR Ama, EDR Nuu and EDR Rya. The cement pastes showed peaks for alite (A), belite (Be), tricalcium aluminate (Ta) and brownmillerite (Br) after one day of hydration, suggesting a higher degree of hydration after one day compared to the paste with the raw MSWI residues. Gypsum (G) and anhydrite (An) peaks were identified after 1 day of hydration, which disappeared after 3 days of hydration, implying an excess of gypsum in the early hydration stages. After the EDR treatment, the MSWI residues contained gypsum and bassanite. The blended pastes may, therefore, contain more gypsum than could react within 1 day. Excess gypsum was not predicted in the thermodynamic modelling, see Fig. 6.

Compared to the raw MSWI residues, the pastes with the treated MSWI residues consistently bound more water than the paste with quartz. Furthermore, the pastes with the treated MSWI residues had a similar portlandite development over time as the raw MSWI residues with some key differences. The pastes with EDR Ama and EDR Nuu had a higher portlandite content after 1 day of hydration than the pastes with raw Ama or raw Nuu. However, it remained lower than the paste with

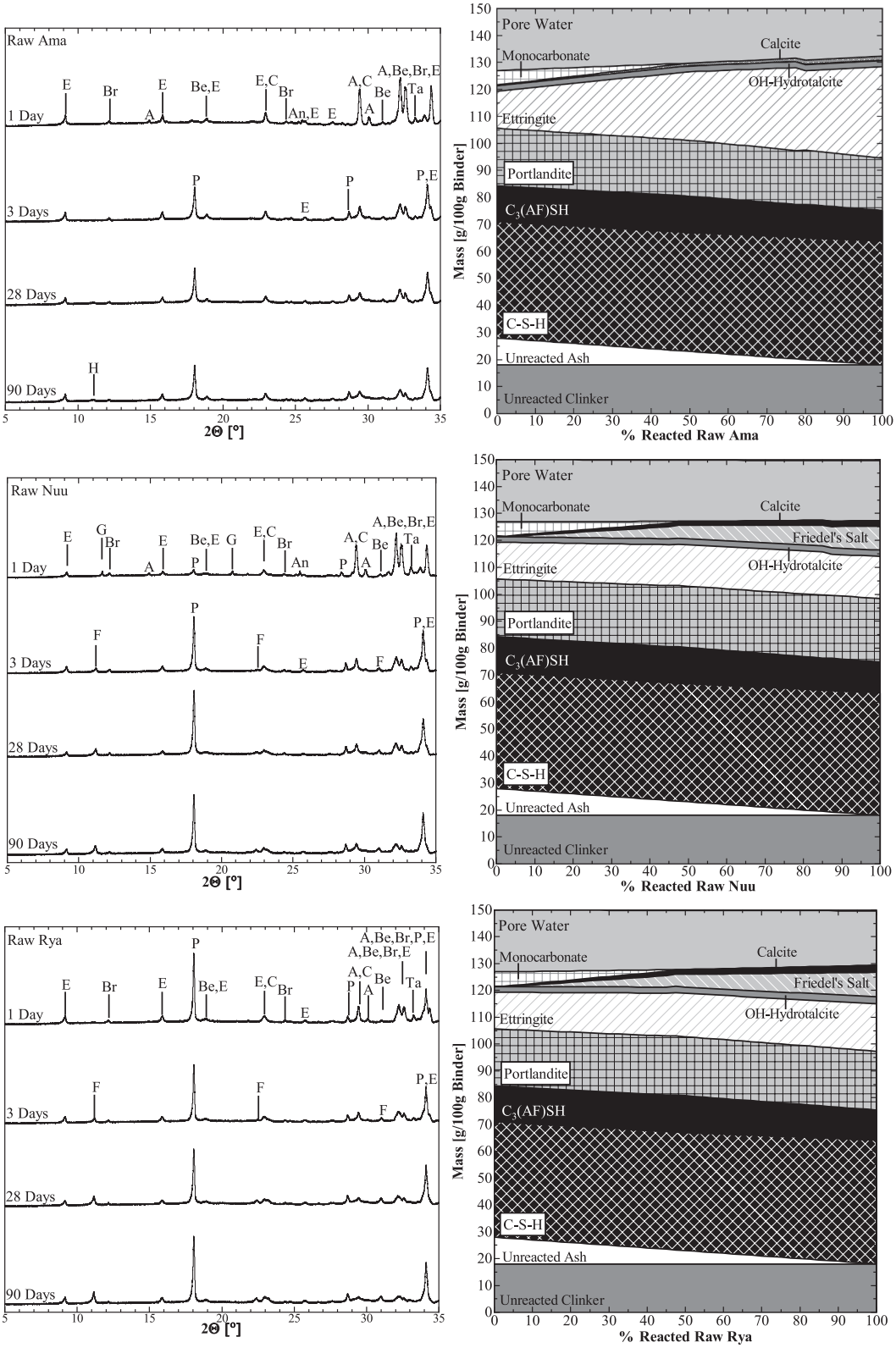

Fig. 5. XRD patterns and thermodynamic modelling of paste with Raw Ama (top), Raw Nuu (middle) and Raw Rya (bottom). Alite (A), belite (Be), tricalcium aluminate (Ta), brownmillerite (Br), portlandite (P), ettringite (E), hemicarbonate (H), Friedel's Salt (F), anhydrite (An), gypsum (G) and calcite (C).

quartz, indicating that EDR Ama and EDR Nuu may still inhibit hydration to a degree. The EDR treatment also changed the phases developing in the pastes. Cement paste with EDR Nuu or EDR Rya developed hemicarbonate (H) after 3 days and monocarbonate (M) after 28 days, similar to the CEM I and Qua paste, instead of Friedel's salt (F), which was seen for the raw MSWI residues. Thermodynamic modelling corroborates this, as monocarbonate is now present with ettringite, regardless of the amount of reacted MSWI residue. Therefore, it is impossible to estimate the amount of reacted EDR Nuu or EDR Rya via the previously used method. The paste with EDR Ama developed

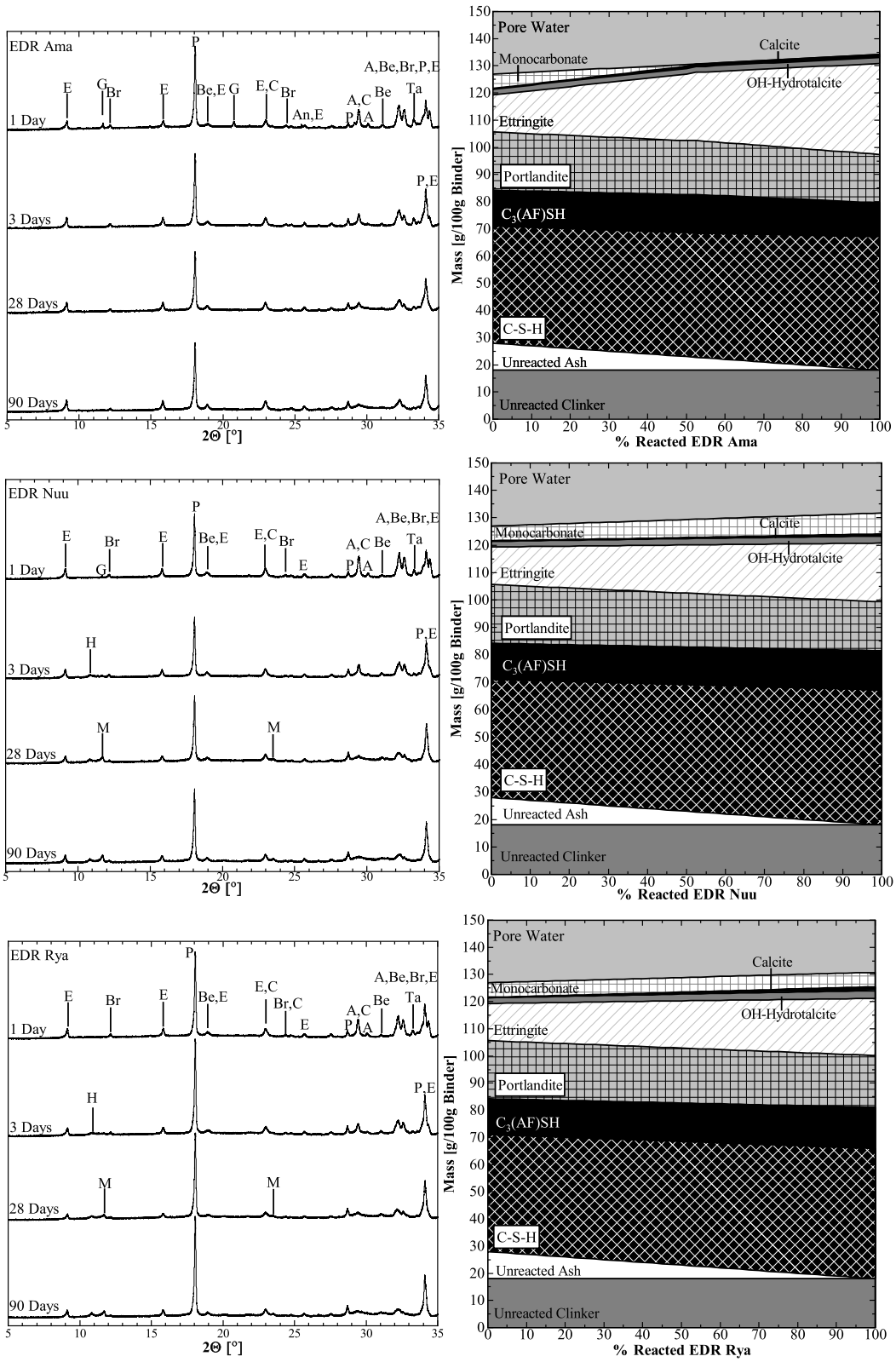

Fig. 6. XRD patterns and thermodynamic modelling of paste with EDR Ama (top), EDR Nuu (middle) and EDR Rya (bottom). Alite (A), belite (Be), tricalcium aluminate (Ta), brownmillerite (Br), portlandite (P), ettringite (E), hemicarbonate (H), monocarbonate (M), anhydrite (An), gypsum (G) and calcite (C).

similarly to paste with Raw Ama, except hemicarbonate were no longer detected, with ettringite (E) being the only AFt/AFm phase observed, attributed to EDR Ama's low Al_2O_3 concentration and high SO_3 concentration compared to the other MSWI residues. The thermodynamic modelling results show a similar development, and together the tests indicate that more than 35 % of EDR Ama has reacted as monocarbonate was not detected in the paste by XRD. The increased bound water observed in the paste with the treated MSWI residues could be due to an increased ettringite and monocarbonate content the more the MSWI residues react. In the pastes with treated MSWI residue, the

thermodynamic modelling showed an increase in C-S-H and a decrease in portlandite due to the increased SiO_2 content in the ashes. However, as evidenced by the Frattini test, the treated MSWI residues reactivity appears to be slow, suggesting this may only be achievable after extended hydration.

3.3. Setting time

The initial and final setting times measured for the various cement pastes are shown in Fig. 7. The setting time test results showed that the CEM I paste had an initial set (column bottom) after 5 h, while the final set (column top) occurred after 10 h. Substituting 10 wt% cement with quartz resulted in a slightly faster initial set (4.8 h), which may be due to the inert quartz having a filler effect [64]. However, the inert quartz has a larger particle size distribution than the cement, see Table 2, suggesting the acceleration may be due to a dilution effect [7].

The impact of the differences in hydration and phase development observed between the treated and raw MSWI residues were apparent for the setting time and compressive strength (section 3.4). Treating the MSWI residues reduced the initial and final setting time delay of Raw Ama by 20 and 25 h and Raw Nuu by 19 and 24 h, respectively, conforming with the CEM I and Qua paste setting. In contrast, the treatment did not improve the setting of the paste with Raw Rya. The cement paste with Raw Rya had an accelerated initial set, occurring after 4 h and an extended final set by 2 h, compared to the CEM I and Qua paste. EDR Rya delayed the initial setting to after 5 h and extended the final set by 1 h. As suggested by the initial clinker phases' peak intensities, bound water and portlandite content, cement pastes with Raw Ama or Raw Nuu do not hydrate and set within 24 h. As previously discussed, this may be attributed to the relative amount of heavy metals in the MSWI residues. Fig. 8a depicts the total concentration of Cd, Cr, Cu, Pb and Zn as mol/kg binder in the cement pastes, together with the concentration of 0.18 mol/kg used in [8], at which a delayed setting was observed. The cement pastes with Raw Ama and Raw Nuu had the highest concentration of metals in the paste and the most extended delay in the initial and final setting. Raw Rya contained a lower relative amount of heavy metals than the other MSWI residues. At low concentrations, Zn and Pb may improve setting [55,57], which, together with its other potentially accelerative components, could be why Raw Rya had a faster initial set and delayed final set. The treated MSWI residues still had a high concentration of heavy metals. The improved setting time could result from differences in metal leachability. As shown in Fig. 8b, the EDR treated MSWI residues have a lower leachable metal content than the raw MSWI residues. The treated MSWI residues also contained gypsum or bassanite, which may extend the induction period [48] and account for the treated MSWI residues delay in the initial setting time.

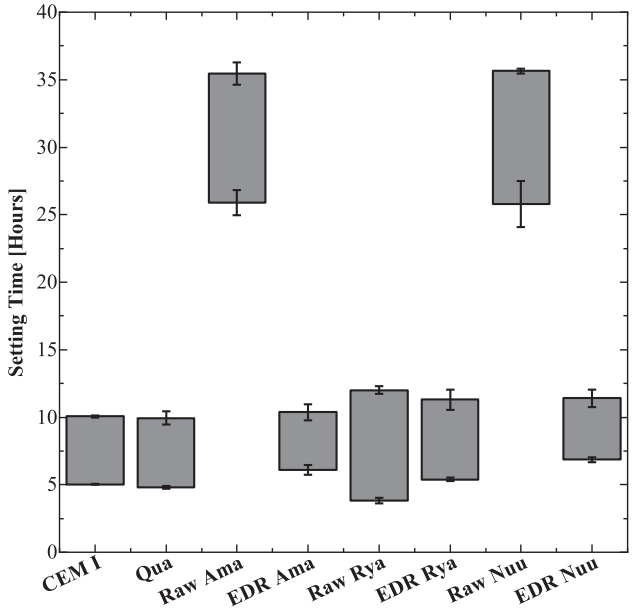

Fig. 7. Initial and final setting times. The error bars indicate standard variation.

3.4. Assessment of mechanical properties

The calculated macroporosity of the tested mortar prisms is shown in Fig. 9. The EDR treatment improved the macroporosity of the mortars. EDR Ama and EDR Rya resulted in macroporosities of 0.7 and 0.3 % (similar to the Qua mortar), while Raw Ama and Raw Rya resulted in macroporosities of 1.2 and 1.1 %, respectively. The most significant improvement was for Raw Nuu, as mortar prisms with Raw Nuu had a macroporosity of 8.3%, while prisms with EDR Nuu had a macroporosity of 1.2 %. The substantially higher macroporosity increase in Raw Nuu mortar may be due to metallic aluminium. A high concentration of metallic aluminium is likely in Greenlandic MSWI fly ash, as metal from household waste is not commonly separated [65]. At high pH, metallic aluminium dissolves according to the following reaction [9]:

$$2Al_{(s)} + 2OH^{-}_{(aq)} = 2Al_2O^{-}_{(aq)} + 2H_{2(g)}$$

Dihydrogen gas release leads to gaseous inclusions, expanding the volume of fresh pastes and potentially cracking the mortar. Such expansion was observed in the mortar prisms with Raw Nuu, with the mortar expanding out of the moulds. However, the concentration of metallic aluminium was not measured. The EDR treatment may have reduced the concentration of metallic aluminium by extracting the aluminium or causing the previously described reactions. Raw Ama and Raw Rya may contain traces of metallic aluminium, which could account for the increased macroporosity. Heavy metals such as Pb and Zn may also increase the pore structure and volume [57,66] of mortar and could be the reasons for the MSWI residue's effect on macroporosity.

The mortar prisms' compressive strength (normalised) is shown in Fig. 10a as a function of time and in Fig. 10b as a function of bound water. The compressive strength test of the mortar with quartz showed that a 10% substitution with an inert material reduced the mortar's compressive strength by 14% after 1 to 3 days of curing and 21–23% after 28 and 90 days of curing. The lower difference in strength between the CEM I and Qua mortar after 1 to 3 days of curing compared to 28 and 90 days may result from the accelerated setting time.

For the two investigated MSWI fly ashes (Ama and Nuu), the EDR treatment vastly improved the compressive strength of the mortar. This was, however, not the case for Rya. After 1 day of curing, the compressive strength of the mortars with the treated MSWI residues was lower than the mortar with quartz, and after three days, it was higher than or equal to the mortar with quartz, except for mortar with EDR Ama. The treated MSWI residues did result in a delayed set attributed to the MSWI residues gypsum or bassanite content, prolonging the induction period (see Section 3.2 and 3.3). EDR Ama had a higher sulphite content than the other MSWI residues, which may have inhibited the early age strength. Although the early age compressive strength of the mortar with the treated MSWI residues was less than mortar with quartz, it does represent an improvement. The delayed cement paste hydration (see Section 3.2 and 3.3) in samples with Raw Ama or Raw Nuu resulted in compressive strength of less than 1 MPa. After three days of curing, the improvement from electrodialytically treating the MSWI residues was more discernable. The mortar with treated MSWI residues achieved compressive strengths between 70 and 75 MPa after 90 days, 10 MPa more than mortar with quartz, while mortar with Raw Ama had a compressive strength of 10 MPa lower than the mortar with quartz. After 90 days, the mortar with Raw Nuu did achieve a similar compressive strength as the mortar with quartz. However, the actual measured compressive strength is less than the mortar with quartz. Treating Raw

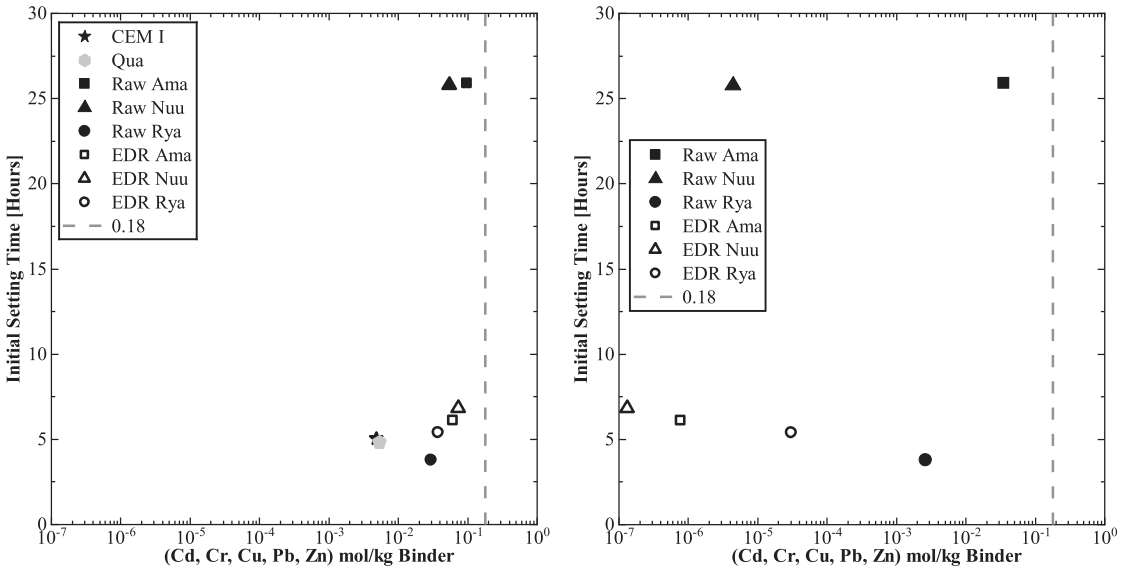

Fig. 8. Initial setting time versus (a) total metal content in the cement paste samples (b) and leachable metals in the cement paste samples. The dashed line is 0.18 mol/kg binder, as used in [7].

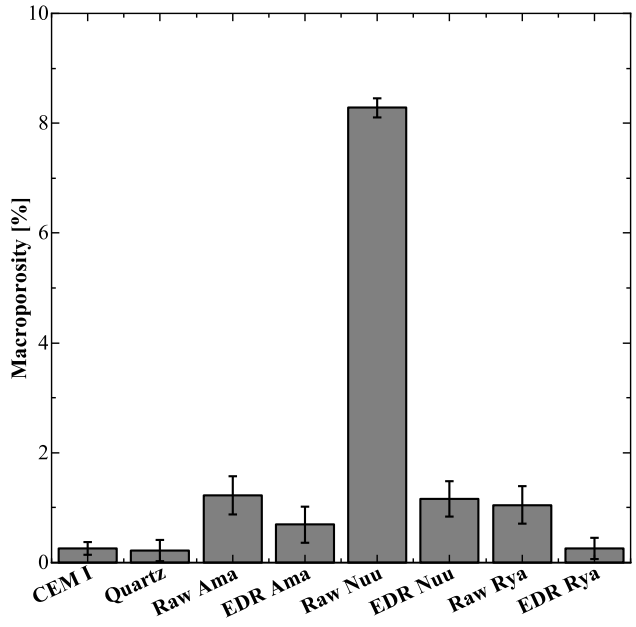

Fig. 9. Calculated average macroporosity of mortar samples.

Rya did not improve the compressive strength development, despite the composition and phase development changes. Mortar with Raw Rya had a compressive strength similar to the CEM I mortar at all of the tested dates, which may be due to the accelerated initial set and high bound water content. The cement paste with EDR Rya had a higher bound water content than the paste with Raw Rya but lower compressive strength, the reason for this is not clear. The EDR treated MSWI residues had a higher bound water content than paste with quartz and CEM I paste but lower compressive strength than the 100 wt% CEM I mortar. The higher bound water content is attributed to a higher ettringite and monocarbonate content in the samples, resulting in a higher compressive strength than the mortar with quartz. While the other raw or treated MSWI residues may inhibit early C-S-H formation, Raw Rya may promote C-S-H formation, therefore, achieving a similar strength to the CEM I mortar.

4. Conclusions

The impact of electrodialytic remediation (EDR) of MSWI fly ash/air pollution control (APC) residue on cement hydration and the development of mechanical properties (setting and compressive strength) were investigated for two MSWI fly ash samples and one MSWI APC residue. The performance was investigated for 10% Portland cement replacement and compared to mixtures with an inert material (quartz).

EDR reduced the initial setting time of blended cement pastes with the two MSWI fly ashes from 25 to 6 h and the final setting time from 35 to 12 h; the improved performance was attributed to the removal of retarding components such as heavy metals. Furthermore, EDR reduced the macroporosity and volume expansion, which was high for especially blended mortars of one of the untreated MSWI fly ashes; this might be explained by a high amount of metallic aluminium resulting in gas evolution.

Combined XRD and thermodynamic modelling showed the relative increase of ettringite and monocarbonate in the phase assemblage. They indicated that approximately 35% of one of the EDR treated MSWI fly ashes reacted in the blended cement paste. Limited change of phase assemblage for the two other MSWI residues did not allow a similar assessment. The contribution seems to be hydraulic as the investigated samples showed no pozzolanic reactivity.

EDR increased the compressive strength of blended, Portland cement-based mortars compared to a mortar with quartz, indicating that all MSWI residues reacted to some extent. The untreated MSWI APC residue also contributed positively to strength development. The two untreated MSWI fly ashes resulted in lower strength development than the mortar with quartz; the reason for the positive behaviour of the untreated MSWI APC residue requires further investigation.

The results indicate that electrodialytic remediation improves the performance of MSWI fly ash in Portland cement-based materials, while MSWI APC residues might be used without pre-treatment.

CRediT authorship contribution statement

Benjamin A.R. Ebert: Conceptualization, Investigation, Methodology, Formal analysis, Writing – original draft. **Mette R. Geiker:** Conceptualization, Writing – review & editing. **Wolfgang Kunther:** Conceptualization, Writing – review & editing. **Gunvor M. Kirkelund:** Conceptualization, Methodology, Supervision, Writing – review &

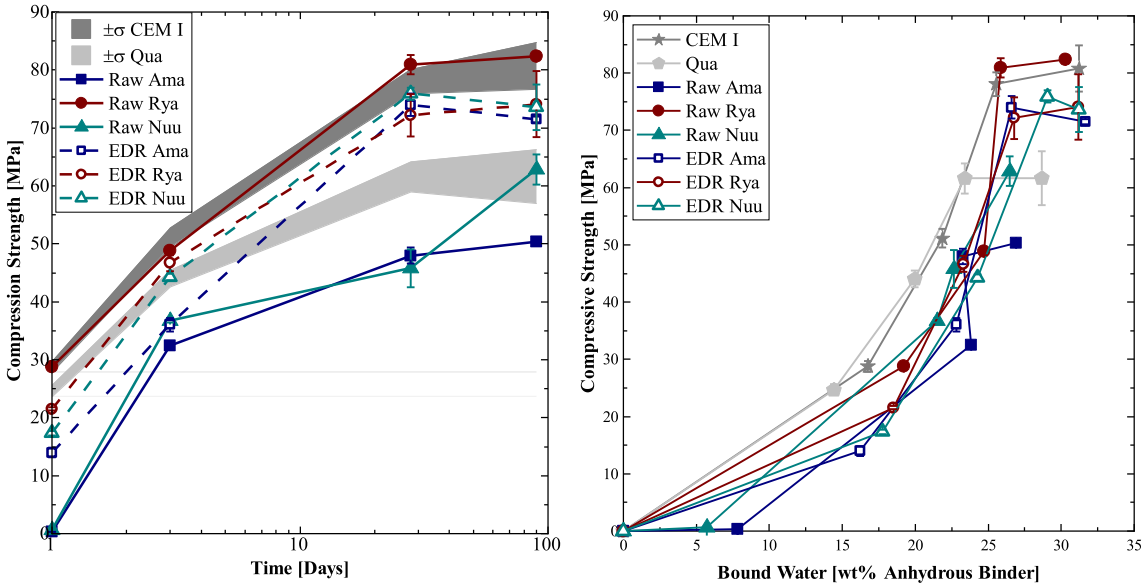

Fig. 10. Compressive strength (normalised to air free) as a function of time and bound water. Error bars and grey areas indicate +/- one.

editing.

Declaration of Competing Interest

The authors declare that they have no known competing financial interests or personal relationships that could have appeared to influence the work reported in this paper.

Acknowledgements

This paper and the research behind it would not have been possible if not for the lab technicians Ebba Schnell, Natasja Due and Erasmus + scholarship recipient Nuria Bernárdez Rodas who helped to conduct and maintain the bench-scale electrodialytic remediation experiments, treating the MSWI fly ash used in this study. The lab technicians are further acknowledged for their assistance with several measurements used in this paper. The people working at Amager Resource Center, Borås Energi och Miljö and Kommuneqarfik Semersooq are also recognised for their interest in the study, their cooperation, and sampling and sending the MSWI fly ash to the Technical University of Denmark.

References

[1] Jos G.J. Olivier; Greet Janssens-Maenhout; Marilena Muntean; Jeroen A.H.W. Peters, Trends in global CO2 emissions 2016, (2016) 86.
[2] K.L. Scrivener, V.M. John, E.M. Gartner, Eco-efficient cements: Potential, economically viable solutions for a low-CO2, cement-based materials industry, (2016).
[3] C. Ferreira, A. Ribeiro, L. Ottosen, Possible applications for municipal solid waste fly ash, J. Hazard. Mater. 96 (2-3) (2003) 201–216.
[4] O. Hjelmar, Disposal strategies for municipal solid waste incineration residues, J. Hazard. Mater. 47 (1-3) (1996) 345–368, https://doi.org/10.1016/0304-3894(95)00111-5.
[5] F. Zunino, D.P. Bentz, J. Castro, Reducing setting time of blended cement paste containing high-SO3 fly ash (HSFA) using chemical/physical accelerators and by fly ash pre-washing, Cem. Concr. Compos. 90 (2018) 14–26, https://doi.org/10.1016/j.cemconcomp.2018.03.018.
[6] S. Kumar, C.V.S.K. Rao, Effect of sulfates on the setting time of cement and strength of concrete, Cement and Concrete Research. 26 (1996) 643. https://doi.org/Doi 10.1016/S0008-8846(96)90013-7.
[7] C.A.A. Rocha, G.C. Cordeiro, R.D. Toledo Filho, Use of thermal analysis to determine the hydration products of oil well cement pastes containing NaCl and KCl, J. Therm. Anal. Calorim. 122 (3) (2015) 1279–1288, https://doi.org/10.1007/s10973-015-4949-6.
[8] N. Gineys, G. Aouad, D. Damidot, Managing trace elements in Portland cement - Part I: Interactions between cement paste and heavy metals added during mixing as soluble salts, Cem. Concr. Compos. 32 (8) (2010) 563–570, https://doi.org/10.1016/j.cemconcomp.2010.06.002.
[9] J.E. Aubert, B. Husson, A. Vaquier, Metallic aluminum in MSWI fly ash: Quantification and influence on the properties of cement-based products, Waste Manage. 24 (6) (2004) 589–596, https://doi.org/10.1016/j.wasman.2004.01.005.
[10] P. Piantone, F. Bodénan, R. Derie, G. Depelsenaire, Monitoring the stabilization of municipal solid waste incineration fly ash by phosphation: Mineralogical and balance approach, Waste Manage. 23 (3) (2003) 225–243, https://doi.org/10.1016/S0956-053X(01)00058-7.
[11] Z. Jing, X. Ran, F. Jin, E.H. Ishida, Hydrothermal solidification of municipal solid waste incineration bottom ash with slag addition, Waste Manage. 30 (8-9) (2010) 1521–1527, https://doi.org/10.1016/j.wasman.2010.03.024.
[12] M.-G. Li, C.-J. Sun, S.-H. Gau, C.-J. Chuang, Effects of wet ball milling on lead stabilization and particle size variation in municipal solid waste incinerator fly ash, J. Hazard. Mater. 174 (1-3) (2010) 586–591, https://doi.org/10.1016/j.jhazmat.2009.09.092.
[13] Z. Yang, S. Tian, R. Ji, L. Liu, X. Wang, Z. Zhang, Effect of water-washing on the co-removal of chlorine and heavy metals in air pollution control residue from MSW incineration, Waste Manage. 68 (2017) 221–231, https://doi.org/10.1016/j.wasman.2017.06.039.
[14] K. HUANG, K. INOUE, H. HARADA, H. KAWAKITA, K. OHTO, Leaching behavior of heavy metals with hydrochloric acid from fly ash generated in municipal waste incineration plants, Transactions of Nonferrous Metals Society of China (English Edition). 21 (6) (2011) 1422–1427, https://doi.org/10.1016/S1003-6326(11)60876-5.
[15] K. WANG, K. CHIANG, J. PERNG, C. SUN, The characteristics study on sintering of municipal solid waste incinerator ashes, J. Hazard. Mater. 59 (2-3) (1998) 201–210, https://doi.org/10.1016/S0304-3894(97)00147-7.
[16] S.-Y. Chou S.-L. Lo C.-H. Hsieh C.-L. Chen Sintering of MSWI fly ash by microwave energy 163 1 2009 357 362 10.1016/j.jhazmat.2008.06.100.
[17] J.E. Aubert, B. Husson, A. Vaquier, Use of municipal solid waste incineration fly ash in concrete, Cem. Concr. Res. 34 (6) (2004) 957–963, https://doi.org/10.1016/j.cemconres.2003.11.002.
[18] K.L. Lin, K.S. Wang, B.Y. Tzeng, C.Y. Lin, The reuse of municipal solid waste incinerator fly ash slag as a cement substitute, Resour. Conserv. Recycl. 39 (4) (2003) 315–324, https://doi.org/10.1016/S0921-3449(02)00172-6.
[19] T. Lenormand, E. Rozière, A. Loukili, S. Staquet, Incorporation of treated municipal solid waste incineration electrostatic precipitator fly ash as partial replacement of Portland cement: Effect on early age behaviour and mechanical properties, Constr. Build. Mater. 96 (2015) 256–269, https://doi.org/10.1016/j.conbuildmat.2015.07.171.
[20] Z. Chen, S. Lu, M. Tang, J. Ding, A. Buekens, J. Yang, Q. Qiu, J. Yan, Mechanical activation of fly ash from MSWI for utilization in cementitious materials, Waste Manage. 88 (2019) 182–190, https://doi.org/10.1016/j.wasman.2019.03.045.
[21] G.M. Kirkelund, P.E. Jensen, Electrodialytic treatment of Greenlandic municipal solid waste incineration fly ash, Waste Manage. 80 (2018) 241–251, https://doi.org/10.1016/j.wasman.2018.09.019.
[22] W. Chen, G.M. Kirkelund, P.E. Jensen, L.M. Ottosen, Electrodialytic extraction of Cr from water-washed MSWI fly ash by changing pH and redox conditions, Waste Manage. 71 (2018) 215–223, https://doi.org/10.1016/j.wasman.2017.09.035.
[23] C. Dias-Ferreira, G.M. Kirkelund, P.E. Jensen, The influence of electrodialytic remediation on dioxin (PCDD/PCDF) levels in fly ash and air pollution control residues, Chemosphere 148 (2016) 380–387, https://doi.org/10.1016/j.chemosphere.2016.01.061.
[24] G.M. Kirkelund, M.R. Geiker, P.E. Jensen, Electrodialytically treated MSWI APC residue as substitute for cement in mortar, Nordic Concrete, Research. (2014) 1–16.

[25] B.A.R. Ebert, B.-M. Steenari, M.R. Geiker, G.M. Kirkelund, Screening of untreated municipal solid waste incineration fly ash for use in cement-based materials: chemical and physical properties, SN Applied Sciences. 2 (5) (2020), https://doi.org/10.1007/s42452-020-2613-7.
[26] B.A.R. Ebert, Valorization of MSWI Fly Ash for Use in Cement-Based Materials, PhD Thesis, Technical University of Denmark, Department of Civil Engineering, 2021.
[27] Á. Fernández, B. Lothenbach, M.C. Alonso, J.L. García Calvo, Thermodynamic modelling of short and long term hydration of ternary binders. Influence of Portland cement composition and blast furnace slag content, Constr. Build. Mater. 166 (2018) 510–521, https://doi.org/10.1016/j.conbuildmat.2018.02.007.
[28] S. Rémond, D.P. Bentz, P. Pimienta, Effects of the incorporation of Municipal Solid Waste Incineration fly ash in cement pastes and mortars - II: Modeling, Cem. Concr. Res. 32 (4) (2002) 565–576, https://doi.org/10.1016/S0008-8846(01)00722-0.
[29] M. Keppert, J.A. Siddique, Z. Pavlík, R. Černý, Wet-Treated MSWI Fly Ash Used as Supplementary Cementitious Material, Adv. Mater. Sci. Eng. 2015 (2015) 1–8, https://doi.org/10.1155/2015/842807.
[30] X. Li, Z. Yu, B. Ma, B. Wu, Effect of MSWI fly ash and incineration residues on cement performances, Journal Wuhan University of Technology, Materials Science Edition. 25 (2) (2010) 312–315, https://doi.org/10.1007/s11595-010-2312-0.
[31] K.-L. Lin, D.F. Lin, W.J. Wang, C.C. Chang, T.C. Lee, Pozzolanic reaction of a mortar made with cement and slag vitrified from a MSWI ash-mix and LED sludge, Constr. Build. Mater. 64 (2014) 277–287, https://doi.org/10.1016/j.conbuildmat.2014.04.088.
[32] K.-S. Wang, K.-L. Lin, Z.-Q. Huang, Hydraulic activity of municipal solid waste incinerator fly-ash-slag-blended eco-cement, Cem. Concr. Res. 31 (1) (2001) 97–103, https://doi.org/10.1016/S0008-8846(00)00423-3.
[33] DS/EN 196-1 2005 Metoder til prøvning af cement – Del 1: Styrkebestemmelse Methods of testing cement – Part 1: Determination of strength, (2016).
[34] DS, EN, 12457–1: Characterisation of waste - Leaching - Compliance test for leaching of granular waste materials and sludges - Part 1: One stage batch test at a liquid to solid ratio of 2 l/kg for materials with high solid content and with particle size bel, Dansk Standard (2002).
[35] DS, EN, 196–5: Methods of testing cement - Part 5: Pozzolanicity test for pozzolanic cement, Dansk Standard (2011).
[36] DS, EN 196, 3 + A1: Methods of testing cement - Part 3: Determination of setting times and soundness, Dansk Standard (2009).
[37] B. Lothenbach, P. Durdzinski, K. de Weerdt, Thermogravimetric Analysis, in: K. Scrivener, R. Snellings, B. Lothenbach (Eds.), A Practical Guide to Microstructural Analysis of Cementitious Materials, CRC Press, 2016, pp. 177–213.
[38] Dmitrii A. Kulik Thomas Wagner Svitlana V. Dmytrieva Georg Kosakowski Ferdinand F. Hingerl Konstantin V. Chudnenko Urs R. Berner GEM-Selektor geochemical modeling package: Revised algorithm and GEMS3K numerical kernel for coupled simulation codes 10.1007/s10596-012-9310-6.
[39] B. Lothenbach, D.A. Kulik, T. Matschei, M. Balonis, L. Baquerizo, B. Dilnesa, G. D. Miron, R.J. Myers, Cemdata18: A chemical thermodynamic database for hydrated Portland cements and alkali-activated materials, Cem. Concr. Res. 115 (2019) 472–506, https://doi.org/10.1016/j.cemconres.2018.04.018.
[40] D.A. Kulik, Improving the structural consistency of C-S-H solid solution thermodynamic models, Cem. Concr. Res. 41 (5) (2011) 477–495, https://doi.org/10.1016/j.cemconres.2011.01.012.
[41] DS/EN 1015-3: Methods of test for mortar for masonry - Part 3: Determination of consistence of fresh mortar (by flow table), Dansk Standard, 1999.
[42] B. Osbæck, The influence of Air content by Assessing the pozzolanidc activity of fly ash by strength testing, Cem. Concr. Res. 15 (1985) 53–64.
[43] DS, EN, 450–1: Fly ash for concrete - Part 1: Definition, Specification and conformity criteria, Dansk Standard (2012).
[44] H. Justnes, Influence of SCMs on hydration and durability of blended cements - Chemical and Physical Principles, Journal of the Chinese Ceramic Society. 13 (2554) 1359–1371.
[45] B. Lothenbach, K. Scrivener, R.D. Hooton, Supplementary cementitious materials, Cem. Concr. Res. 41 (12) (2011) 1244–1256, https://doi.org/10.1016/j.cemconres.2010.12.001.
[46] M. Thomas, Supplementary Cementing Materials in Concrete, CRC Press, 2013.
[47] H.-sheng. Shi, L.-li. Kan, Characteristics of municipal solid wastes incineration (MSWI) fly ash-cement matrices and effect of mineral admixtures on composite system, Constr. Build. Mater. 23 (6) (2009) 2160–2166, https://doi.org/10.1016/j.conbuildmat.2008.12.016.
[48] B. Mota, T. Matschei, K. Scrivener, S. Kumar, C.V.S.K. Rao, The influence of sodium salts and gypsum on alite hydration, Cem. Concr. Res. 75 (2015) 53–65, https://doi.org/10.1016/j.cemconres.2015.04.015.
[49] I. Jawed, J. Skalny, Alkalis in cement: A review II, Effects of Alkalies on Hydration and Performance of Portland Cement, Cement and Concrete Research. 32 (1978) 147–156.
[50] D.P. Bentz, F. Zunino, D. Lootens, Chemical vs. Physical Acceleration of Cement Hydration, Concrete International : Design & Construction. 38 (2016) 37–44.
[51] T. Vehmas, A. Kronlöf, A. Cwirzen, Calcium chloride acceleration in ordinary Portland cement, Mag. Concr. Res. 70 (16) (2018) 856–863, https://doi.org/10.1680/jmacr.17.00079.
[52] V.S. Ramachandran, Calcium chloride in concrete- applications and ambiguities, Can. J. Civ. Eng. 5 (2) (1978) 213–221.
[53] F.R. Lago, J. Dweck, T. Analysis, Evaluation of Influence of Salt in the Cement Hydration to Oil Wells 20 (2017) 743–747.
[54] M. Zajac, A. Rossberg, G. le Saout, B. Lothenbach, Influence of limestone and anhydrite on the hydration of Portland cements, Cem. Concr. Compos. 46 (2014) 99–108, https://doi.org/10.1016/j.cemconcomp.2013.11.007.
[55] S. Komarneni, E. Breval, D.M. Roy, R. Roy, Reactions of some calcium silicates with metalcations, Cem. Concr. Res. 18 (2) (1988) 204–220.
[56] T. Mangialardi, A.E. Paolini, A. Polettini, P. Sirini, Optimization of the solidification/stabilization process of MSW fly ash in cementitious matrices, J. Hazard. Mater. 70 (1-2) (1999) 53–70, https://doi.org/10.1016/S0304-3894(99)00132-6.
[57] B. Cohen, J. Petrie, Containment of chromium and zinc in ferrochromium flu dusts by cement-based solidification, Can. Metall. Q. 36 (1997) 251–260, https://doi.org/10.1081/E-EEE2-120046011.
[58] D.L. Cocke, The binding chemistry and leaching mechanisms of hazardous substances in cementitious solidification/stabilization systems, J. Hazard. Mater. 24 (2-3) (1990) 231–253, https://doi.org/10.1016/0304-3894(90)87013-8.
[59] F.K. Cartledge, L.G. Butler, D. Chalasani, H.C. Eaton, F.P. Frey, E. Herrera, M. E. Tittlebaum, S.L. Yang, Immobilization Mechanisms in Solidification/Stabilization of Cd and Pb Salts Using Portland Cement Fixing Agents, Environ. Sci. Technol. 24 (1990) 867–873, https://doi.org/10.1021/es00076a012.
[60] C.S. Poon, A.I. Clark, C.J. Peters, R. Perry, Mechanisms of metal Fixation and leaching by cement based fixation processes, Waste Manage. Res. 3 (1985) 127–142, https://doi.org/10.1016/0048-9697(85)90161-5.
[61] A. Vollpracht, W. Brameshuber, Binding and leaching of trace elements in Portland cement pastes, Cem. Concr. Res. 79 (2016) 76–92, https://doi.org/10.1016/j.cemconres.2015.08.002.
[62] B. Lothenbach, G. Le Saout, E. Gallucci, K. Scrivener, Influence of limestone on the hydration of Portland cements, Cem. Concr. Res. 38 (6) (2008) 848–860, https://doi.org/10.1016/j.cemconres.2008.01.002.
[63] T. Matschei, B. Lothenbach, F.P. Glasser, The role of calcium carbonate in cement hydration, Cem. Concr. Res. 37 (4) (2007) 551–558, https://doi.org/10.1016/j.cemconres.2006.10.013.
[64] K.L. Scrivener, B. Lothenbach, N. de Belie, E. Gruyaert, R. Snellings, A. Vollpracht, TC 238-SCM : hydration and microstructure of concrete with SCMs State of the art on methods to determine degree of reaction of SCMs, (2015) 835–862. https://doi.org/10.1617/s11527-015-0527-4.
[65] R. Eisted, T.H. Christensen, Waste management in Greenland: Current situation and challenges, Waste Manage. Res. 29 (10) (2011) 1064–1070, https://doi.org/10.1177/0734242X10395421.
[66] F. Sanchez, R. Barna, A. Garrabrants, D.S. Kosson, P. Moszkowicz, Environmental assessment of a cement-based solidified soil contaminated with lead, Chem. Eng. Sci. 55 (1) (2000) 113–128, https://doi.org/10.1016/S0009-2509(99)00281-X.